NANO LETTERS

2007
Vol. 7, No. 7
2108−2111

Ultra-Large Room-Temperature Compressive Plasticity of a Nanocrystalline Metal

D. Pan,[†,‡] S. Kuwano,[†] T. Fujita,[†] and M. W. Chen*[,†,‡]

Institute for Materials Research and Institute for International Advanced Interdisciplinary Research, Tohoku University, Sendai 980-8577, Japan

Received May 10, 2007; Revised Manuscript Received May 24, 2007

ABSTRACT

We report ultra-large room-temperature plasticity of nanocrystalline Ni subjected to uniaxial compression. Up to 200% true plastic strain is achieved with a steady flow stress of ~2 GPa at strain rates ranging from 10^{-3} to 10^{-1} s^{-1}. The low temperature, high strain rate, and high flow stress demonstrate that the observed ultra-large plasticity in nanocrystalline Ni is intrinsically dissimilar to that in traditional superplastic materials deformed at high temperatures. Microstructural observations reveal significant nanograin growth accompanied with the ultra-large plastic deformation, indicating the ultra-large plasticity in nanocrystalline Ni at room temperature is mainly performed by a grain-boundary-mediated process that is driven by high stresses rather than by thermal diffusion.

The capability of certain materials to sustain a very large plastic strain has been intensely studied in metals, ceramics, intermetallics, and composites because of its commercial applications in forming components with complex shapes.[1,2] The ultra-large plasticity often occurs at elevated temperatures above 50% of the melting points of the materials with a slow strain rate (10^{-5}−10^{-4} s^{-1}). In light of this, ultra-large plasticity at low temperatures, in particular at room temperature, and high strain rates (e.g., 10^{-3}−10° s^{-1}) is of particular interests because it can significantly cut down the costs of plastic-forming technology by reducing forming time and lowering forming temperatures.[1,3−5] Generally, ultra-large plastic flow of a material is associated with its grain boundary (GB) activities, and smaller grains promote the ultra-large plastic flow at lower temperatures and higher strain rates.[1] Thus, as a reasonable extrapolation, room-temperature ultra-large plastic deformation of nanocrystalline metals, which possess a characteristic grain size less than 100 nm, had been expected many years ago.[6] Although superplastic flow of nanocrystalline nickel (nc NI) has been reported at a relative low-temperature range from 350 °C to 420 °C,[5] the room-temperature ultra-large plastic flow of nanocrystalline metals has not been proved by definitive experiments and is even in conflict with the broad observations that nanocrystalline metals often fail at a tensile strain typically less than 2%.[7−10] Several ways to simultaneously sustain large plasticity and high strength of nanostructured materials have been proposed;[11−14] however, whether the ultra-large plastic flow of nanocrystalline metals can be intrinsically sustained at room-temperature still remains unclear.

nc Ni films with a thickness of ~200 μm were prepared by electrodeposition. Transmission electron microscope (TEM) observations revealed that the as-deposited nc Ni films are fully dense with an average nanograin size of ~20 nm (Figure 1a). Most of the nanograins were found to be separated by high-angle GBs whereas GB phases (e.g., amorphous films) have not been seen (Figure 1b). Chemical analysis performed by atom probe tomography suggested that the nc Ni is of high purity and only trace impurity elements (30−100 ppm), mainly Fe and S, uniformly distribute in nanograins. Detectable GB segregations have not been observed. Compression testing of the nc Ni was performed by a newly developed micro-compression technique.[15] The micropillars with nominal diameters ranging from 3 μm to 8 μm and an aspect ratio of 2:1 were prepared by a focused ion beam (FIB) system, following a modification of prototypical methodology by Uchic et al.[15] Fine-milling processes were applied with lower milling currents (e.g., 0.02 nA) thereafter to carefully eliminate the visible tapering of sidewalls of the cylindrical micropillars for accurate measurements of flow stresses of the nc Ni.[16,17] A 44-μm-in-diameter pool where the micropillar resides at the center was designed to provide a sufficient space for the pyramidal indenter during a test. Figure 2a shows a typical micro-pillar of nc Ni with the maximum difference in cross-sectional area along the loading axis no greater than 5%. A nanoindentation apparatus, equipped with a flat-end diamond indenter, was

* Corresponding author. E-mail: mwchen@imr.tohoku.ac.jp. Phone: 81-22-215-2143.
[†] Institute for Materials Research.
[‡] Institute for International Advanced Interdisciplinary Research.

10.1021/nl071093m CCC: $37.00
Published on Web 06/06/2007

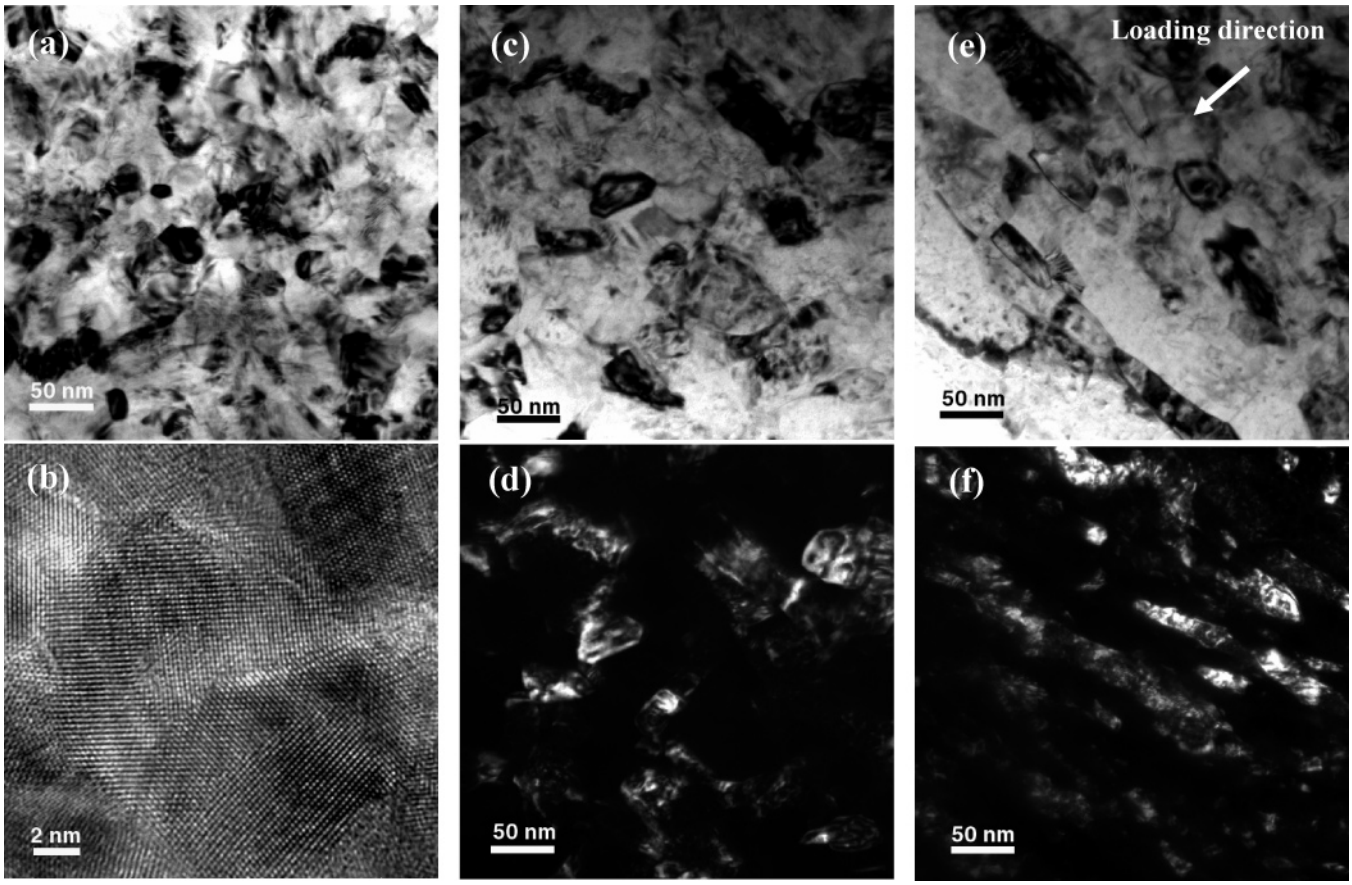

Figure 1. TEM images of microcompression samples with different deformation amounts. (a) As-prepared nc Ni. (b) High-resolution electron micrograph of the as-prepared nc Ni. (c and d) Bright- and dark-field TEM micrographs of the sample with 40% true strain. (e and f) Bright- and dark-field TEM micrographs of the sample with 140% true strain. The compression tests for the imaged specimens were performed at a loading rate of 0.132 mN/s. The extensively deformed nanograins were subjected to severe elongation in the direction perpendicular to the loading axis, as shown in parts e and f.

employed to carry out the room-temperature microcompression tests with loading rates ranging from 0.132 mN/s to 13.2 mN/s (the corresponding strain rates range from 4×10^{-3} s^{-1} to 5.4×10^{-1} s^{-1} during steady plastic flow). Prior to each test, the apparatus was finely tuned and aligned to avoid off-axis loading of the sample. All the load versus deformation curves obtained in the compression tests were converted into true stress versus true strain plots. For convenience, all the compressive stresses and strains referenced herein are expressed in positive values. The micropillars were sliced employing FIB along their axial direction as thin wedges with an electron transparent edge for TEM observations of the pre- and post-deformation pillars. Detectable gallium (ion source) contamination and damage were not found in the TEM specimens through systematic energy dispersive X-ray analysis.

The nc Ni exhibits large compression plasticity with moderately uniform deformation. An example of a microcompression specimen axially strained to a true strain of 50% is presented in Figure 2b. Surprisingly, up to 200% true strain, or 85% loss of its initial height, was obtained in nc Ni without neither material nor structural failure (Figure 2c). Further compression is still possible to enhance the deformation. Moreover, strong diameter dependence of the ultralarge plastic flow of the nc Ni has not been found in a sample diameter range from 3 to 8 μm. At all loading rates, we evidenced ultra-large plastic flow of the nc Ni (>160% true strain without failure) under unidirectional compression at room temperature ($\sim$0.17 T_M of Ni) and high strain rates (10^{-3}–10^{-1} s^{-1}), which was not previously documented in literature. A typical true stress (σ) versus true strain (ϵ) curve of nc Ni strained up to $\sim$100% is shown in Figure 3. Steady flow stresses of 2.0–2.4 GPa, approximately four times the yield strength of coarse-grained Ni, were obtained with loading rates ranging from 0.132 mN/s to 13.2 mN/s, which is consistent with the compressive strength of nc Ni reported in the literature.[18] The ultra-large plastic flow of nc Ni is composed of two stages upon the onset of steady plastic flow, that is, strain softening up to the deformation of about 60% (Regime III) followed by strain hardening (Regime IV). These altering mechanical performances with deformation amounts are found to be associated with the deformation-induced nanostructural evolution. Figure 1c–f show the size and morphology of nanograins in the specimens with various deformation amounts. Visible nanograin growth occurs in the specimens deformed in the steady plastic flow stage and nanograins remain nearly equiaxial with $\sim$40% plastic deformation (Figure 1c,d). The uniform nanograin growth indicates that the steady plastic flow is associated with the stress-assisted GB motion[19–21] along with the intragranular

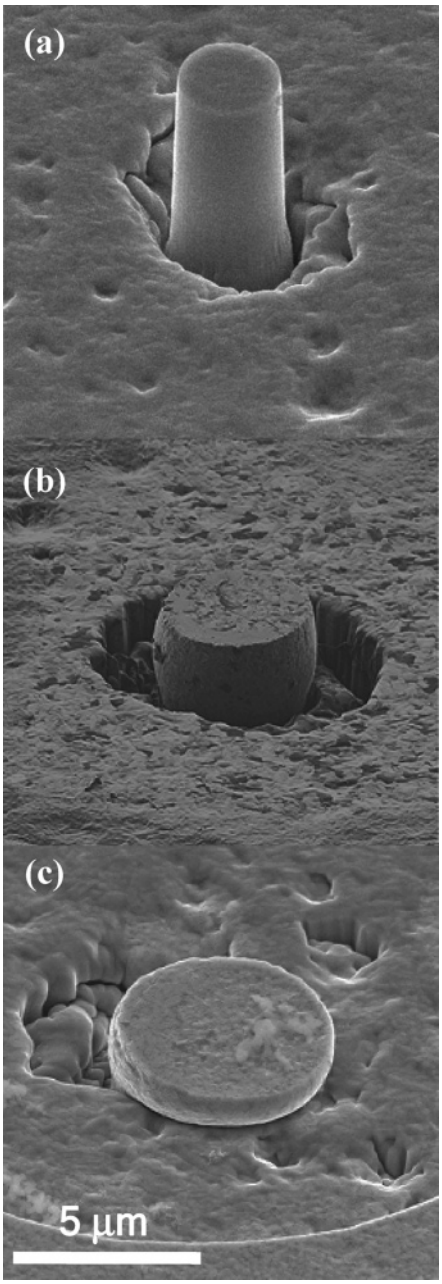

Figure 2. FIB micrographs of microcompression samples with different deformation amounts. (a) As-fabricated. (b) 50% true strain. (c) 200% true strain. No catastrophic failure was observed on the deformed samples. The barreling feature of deformed samples is typical of those fixed at one end when subjected to compression, suggesting a comparatively uniform distribution of plastic deformation.

deformation by twinning and dislocation gliding. Furthermore, the deformation induced nanograin growth can lead to enhanced ductility and obvious strain softening in nanocrystalline metals.[22,23] In contrast, the microscopic images taken from the sample deformed in Regime IV (~140% true strain) (Figure 1e,f) show coarsened and elongated nanograins that contain a high density of dislocations, stacking faults, and deformation twins. Apparently, the deformation in this regime is performed mainly by the intragranular straining of the coarsened nanograins, and, thus, strain hardening takes place. Measurements of coarse-grained

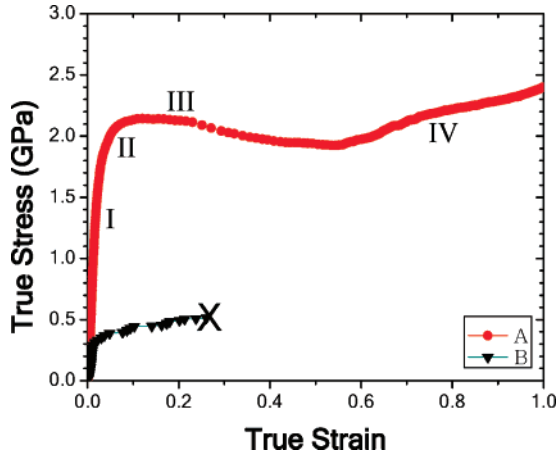

Figure 3. Representative true stress vs true strain curve of nc nickel subjected to microcompression. Four regimes of the mechanical response can be distinguished in a typical true stress vs true strain curve of nc Ni (curve A): Regime I corresponds to elastic deformation of nc Ni; Regime II identifies the initial strain strengthening upon the inception of plastic deformation, which has been extensively observed in tensile tests with limited plasticity;[9,10] Regime III represents the steady plastic flow with strain softening caused by nanograin growth; and Regime IV denotes the steady plastic flow with apparent strain strengthening. By contrast, a typical true stress vs true strain curve of coarse-grained Ni (curve B) demonstrates that the coarse-grained sample fails at true strain less than 30%.

nickel following the same sample fabrication and testing methodology showed that the micro-pillars failed to sustain further loading at a true strain less than 30% (Figure 3). The lack of extended ductility in coarse-grained Ni by microcompression concurs with the well-established conclusion by conventional compression testing, ruling out a methodological effect on the observed ultra-large plastic flow of nc Ni at room temperature.

Although at room temperature and high stress levels diffusion creep was reported to make a significant contribution to deformation of nc Ni, the creep strain is estimated to be no more than 10% even in the case of our lowest loading rate.[24] Molecular dynamics (MD) simulations[25−27] and some experimental observations[28] pointed out that plasticity of nanocrystalline metals is mostly accommodated by GB processes such as GB sliding, in many instances accompanied by partial dislocation activities. Formation of stacking faults and/or deformation twins, albeit observed as evidence of partial dislocation activities,[29,30] is apparently unable to provide such a large amount of plastic deformation as observed in this study. Moreover, MD simulations of uniaxial deformation of nanocrystalline metals[25−27] revealed that GB sliding takes place mainly via a large number of small local sliding events of atomic clusters that comprises a few or at most a few tens of GB atoms. This stress-enhanced mass transport along GBs, in nature, can lead to ultra-large plastic flow in the absence of enough thermal assistance by high temperatures, accompanied by other atomic-scale GB processes such as nucleation of dislocations. The observed ultra-large plastic flow of nc Ni is thus nearly rate-independent because the dominating deformation mechanism, that is, stress-enhanced mobility of GB atoms, mainly depends on

stress levels rather than time in the case of thermally activated GB diffusion, facilitating the ultra-large plastic flow at high strain rates. In addition, this collective atoms motion at GBs predicted by MD simulations fairly coincides with the measured activation volumes for ultra-large plastic flow and deformation-induced nanograin growth.[31] Accordingly, the nanograin growth and plastic deformation of nc Ni under compression most likely take place simultaneously through stress-enhanced GB motion because both sliding for plastic deformation and migration for nanograin growth are motivated by the mobility or diffusivity of GB atoms.

The typical tensile ductility of nc Ni was reported not to exceed 2%, and most of the fractured tensile specimens loaded at strain rates similar to those in our work showed a post-necking nature.[9,10] The presence of necking in the tensile specimens, associated with the destabilization of uniform plastic flow, is known to give rise to a locally high strain rate ($\dot{\epsilon}$). Therefore, a strain rate sensitivity of flow stress, $m = \partial(\log \sigma)/\partial(\log \dot{\epsilon})$, is the most important material property for tensile plasticity, because high m can bestow a sufficient opposition to neck development by a significant increase in the flow stress within the necked region, and thus leads to superior tensile elongation.[1] For nc Ni, the room-temperature strain rate sensitivity is about $0.02-0.03$.[9,10,23] This value, although considerably higher than that of its coarse-grained Ni ($\sim$0.005),[10] is still much lower than that of traditional superplastic materials, that is, $0.4-0.8$.[1] As a consequence, extended tensile plasticity cannot be attained in nc Ni. However, when under compression, the nanocrystalline metals do not necessarily sustain high strain rate sensitivity as a prerequisite for an ultra-large plastic deformation because necking cannot be manifested in a compression test.

Supporting Information Available: Finite element modeling of uniaxial microcompression, basic composition of the electro-deposition bath and the plating conditions, FIB image of "failed" sample of course-grained Ni by microcompression, and finite element analysis of microcompression testing. This material is available free of charge via the Internet at http://pubs.acs.org.

References

(1) Chokshi, A. H.; Mukherjee, A. K.; Langdon, T. G. Superplasticity in advanced materials. *Mater. Sci. Eng., R* **1993**, *10*, 237.

(2) Zhan, G. D.; Garay, J. E.; Mukherjee, A. K. Ultralow-temperature superplasticity in nanoceramic composites. *Nano Lett.* **2005**, *5*, 2593.

(3) Karch, J.; Birringer, R.; Gleiter, H. Ceramics ductile at low-temperature. *Nature* **1987**, *330*, 556.

(4) Kim, B. N.; Hiraga, K.; Morita, K.; Sakka, Y. A high-strain-rate superplastic ceramic. *Nature* **2001**, *413*, 288.

(5) McFadden, S. X.; Mishra, R. S.; Valiev, R. Z.; Zhilyaev, A. P.; Mukherjee, A. K. Low-temperature superplasticity in nanostructured nickel and metal alloys. *Nature* **1999**, *398*, 684.

(6) Gleiter, H. Nanocrystalline materials. *Prog. Mater. Sci.* **1989**, *33*, 223.

(7) Koch, C. C.; Morris, D. G.; Lu, K.; Inoue, A. Ductility of nanostructured materials. *Mater. Res. Soc. Bull.* **1999**, *24*, 54.

(8) Weertman, J. R.; Farkas, D.; Hemker, K. J.; Kung, H.; Mayo, M.; Mitra, R.; Van Swygenhoven, H. Structure and mechanical behavior of bulk nanocrystalline materials. *Mater. Res. Soc. Bull.* **1999**, *24*, 44.

(9) Kumar, K. S.; Van Swygenhoven, H.; Suresh, S. Mechanical behavior of nanocrystalline metals and alloys. *Acta Mater.* **2003**, *51*, 5743.

(10) Chen, M. W.; Ma, E.; Hemker, K. J. In *Nanomaterials Handbook*; Gogotsi, Y., Ed.; Taylor & Francis/CRC Press: Boca Raton, FL, 2006; p 497.

(11) Wang, Y. M.; Chen, M. W.; Zhou, F. H.; Ma, E. High tensile ductility in a nanostructured metal. *Nature* **2002**, *419*, 912.

(12) Farkas, D.; Hyde, B. Improving the ductility of nanocrystalline bcc metals. *Nano Lett.* **2005**, *5*, 2403.

(13) Zhao, Y. H.; Liao, X. Z.; Cheng, S.; Ma, E.; Zhu, Y. T. Simultaneously increasing the ductility and strength of nanostructured alloys. *Adv. Mater.* **2006**, *18*, 2280.

(14) Lu, L.; Wang, L. B.; Ding, B. Z.; Lu, K. High-tensile ductility in nanocrystalline copper. *J. Mater. Res.* **2000**, *15*, 270.

(15) Uchic, M. D.; Dimiduk, D. M.; Florando, J. N.; Nix, W. D. Sample dimensions influence strength and crystal plasticity. *Science* **2004**, *305*, 986.

(16) Uchic, M. D.; Dimiduk, D. M. A methodology to investigate size scale effects in crystalline plasticity using uniaxial compression testing. *Mater. Sci. Eng., A* **2005**, *400*, 268.

(17) Schuster, B. E.; Wei, Q.; Zhang, H.; Ramesh, K. T. Microcompression of nanocrystalline nickel. *Appl. Phys. Lett.* **2006**, *88*, 103112.

(18) Zhao, Y. S.; Zhang, J. Z.; Clausen, B.; Shen, T. D.; Gray, G. T., III; Wang, L. Thermomechanics of nanocrystalline nickel under high pressure-temperature conditions. *Nano Lett.* **2007**, *7*, 426.

(19) Zhang, K.; Weertman, J. R.; Eastman, J. A. Rapid stress-driven grain coarsening in nanocrystalline Cu at ambient and cryogenic temperatures. *App. Phys. Lett.* **2005**, *87*, 061921.

(20) Chen, M. W.; Yan, X. Q. Comment on "grain boundary-mediated plasticity in nanocrystalline nickel". *Science* **2005**, *308*, 356c.

(21) Li, J. C. M. Mechanical grain growth in nanocrystalline copper. *Phys. Rev. Lett.* **2006**, *96*, 215506.

(22) Gianola, D. S.; Van Petegem, S.; Legros, M.; Brandstetter, S.; Van Swygenhoven, H.; Hemker, K. J. Stress-assisted discontinuous grain growth and its effect on the deformation behavior of nanocrystalline aluminum thin films. *Acta Mater.* **2006**, *54*, 2253.

(23) Pan, D.; Nieh, T. G.; Chen, M. W. Strengthening and softening of nanocrystalline nickel during multistep nanoindentation. *Appl. Phys. Lett.* **2006**, *88*, 161922.

(24) Wang, N.; Wang, Z.; Aust, K. T.; Erb, U. Room temperature creep behavior of nanocrystalline nickel produced by an electrodeposition technique. *Mater. Sci. Eng., A* **1997**, *237*, 150.

(25) Schiotz, J.; Di Tolla, F. D.; Jacobsen, K. W. Softening of nanocrystalline metals at very small grain sizes. *Nature* **1998**, *391*, 561.

(26) Van Swygenhoven, H.; Derlet, P. M. Atomic positional disorder in fcc metal nanocrystalline grain boundaries. *Phys. Rev. B* **2001**, *64*, 224105.

(27) Schiotz, J.; Jacobsen, K. W. A maximum in the strength of nanocrystalline copper. *Science* **2003**, *301*, 1357.

(28) Milligan, W. W.; Hackney, S. A.; Ke, M.; Aifantis, E. C. In situ studies of deformation and fracture in nanophase materials. *Nanostruct. Mater.* **1993**, *2*, 267.

(29) Yamakov, V.; Wolf, D.; Phillpot, S. R.; Mukherjee, A. K.; Gleiter, H. Dislocation processes in the deformation of nanocrystalline aluminium by molecular-dynamics simulation. *Nat. Mater.* **2002**, *1*, 45.

(30) Chen, M. W.; Ma, E.; Hemker, K. J.; Sheng, H. W.; Wang, Y. M.; Cheng, X. M. Deformation twinning in nanocrystalline aluminium. *Science* **2003**, *300*, 1275.

(31) We systematically calculated the activation volume for ultra-large plastic flow of the nc Ni by measuring its strain rate sensitivity of flow stress. Meanwhile, the activation volume for deformation induced nanograin growth was determined by measuring the kinetics of nanograin growth. These measurements suggest that the activation volumes for both the ultra-large plastic deformation and the nanograin growth are $\sim 8-20$ atoms, which is fairly consistent with the MD simulations that the GB motion during deformation is performed by the activities of atomic clusters composed of a few or at most a few tens of GB atoms.[25]

NL071093M